Test of self-organization in beach cusp formation

Giovanni Coco,[1] T. K. Burnet, and B. T. Werner

Complex Systems Laboratory, Cecil and Ida Green Institute of Geophysics and Planetary Physics, University of California, San Diego, La Jolla, California, USA

Steve Elgar

Woods Hole Oceanographic Institution, Woods Hole, Massachusetts, USA

[1]   Field observations of swash flow patterns and morphology change are consistent with the hypothesis that beach cusps form by self-organization, wherein positive feedback between swash flow and developing morphology causes initial development of the pattern and negative feedback owing to circulation of flow within beach cusp bays causes pattern stabilization. The self-organization hypothesis is tested using measurements from three experiments on a barrier island beach in North Carolina. Beach cusps developed after the beach was smoothed by a storm and after existing beach cusps were smoothed by a bulldozer. Swash front motions were recorded on video during daylight hours, and morphology was measured by surveying at 3–4 hour intervals. Three signatures of self-organization were observed in all experiments. First, time lags between swash front motions in beach cusp bays and horns increase with increasing relief, representing the effect of morphology on flow. Second, differential erosion between bays and horns initially increases with increasing time lag, representing the effect of flow on morphology change because positive feedback causes growth of beach cusps. Third, after initial growth, differential erosion decreases with increasing time lag, representing the onset of negative feedback that stabilizes beach cusps. A numerical model based on self-organization, initialized with measured morphology and alongshore-uniform distributions of initial velocities and positions of the swash front at the beginning of a swash cycle, reproduces the measurements, except for parts of one experiment, where limited surveys and a significant low-frequency component to swash motions might have caused errors in model initialization.   *INDEX TERMS:* 4546 Oceanography: Physical: Nearshore processes; 4255 Oceanography: General: Numerical modeling; 3022 Marine Geology and Geophysics: Marine sediments—processes and transport; 3220 Mathematical Geophysics: Nonlinear dynamics

1.   Introduction

[2]   Beach cusps are rhythmic patterns in shoreline morphology in the region where breaking waves have collapsed into a thin tongue of water, called swash, that runs up and then down the beach. Beach cusps are characterized by prominent, narrow horns, often tapering seaward to a point, separated by broad, gently curving bays. The alongshore distance between horns or bays typically is 1–50 m and tends to be proportional to the distance swash runs up the beach (swash excursion) or to the square of wave period times beach slope [*Longuet-Higgins and Parkin*, 1962; *Williams*, 1973; *Inman and Guza*, 1982; *Coco et al.*,

1999]. Beach cusps form most readily when narrow-banded waves are normally incident [*Longuet-Higgins and Parkin*, 1962; *Sallenger*, 1979; *Guza and Bowen*, 1981]. Storm waves or strong alongshore currents tend to smooth beach cusps, often as the foreshore erodes [*Russell and McIntire*, 1965; *Miller et al.*, 1989; *Masselink et al.*, 1997].

[3]   Quantitative, predictive models for the formation of beach cusps include (1) formation by imposition of a template of standing waves on the beach [*Komar*, 1973; *Guza and Inman*, 1975; *Inman and Guza*, 1982] and (2) formation by self-organizing feedbacks between flow of swash and morphology [*Werner and Fink*, 1993; *Coco et al.*, 2000]. Additional proposed mechanisms for beach cusp formation include feedbacks between grain size and infiltration [*Longuet-Higgins and Parkin*, 1962; *Dean and Maurmeyer*, 1980], wave refraction [*Kuenen*, 1948], berm breaching [*Dubois*, 1978], and the intersection of obliquely incident waves [*Dalrymple and Lanan*, 1976]. However,

---

[1]Now at National Institute of Water and Atmospheric Research, Hamilton, New Zealand.

quantitative models that would permit tests of these mechanisms have not been developed.

[4] In the standing wave model, the pattern of beach cusps originates with a pre-existing pattern of flow near the shoreline [*Inman and Guza*, 1982; *Komar*, 1973; *Guza and Inman*, 1975]. Edge waves are generated by nonlinear interactions with incident wind waves [*Gallagher*, 1971; *Bowen and Guza*, 1978; *Herbers et al.*, 1995] and are trapped near the shore by the increase of shallow water wave speed with depth [*Ursell*, 1952]. In the presence of dissipation, the fastest growing mode is the subharmonic [*Guza and Davis*, 1974]. For subharmonic edge waves, horns correspond to edge-wave nodes, where swash excursion is minimum, and bays correspond to antinodes, where swash excursion is maximum. For synchronous edge waves, both horns and bays are located at edge wave antinodes. Sand is transported from bay to horn by secondary net currents augmenting first-order sinusoidal motion [*Bowen and Inman*, 1971].

[5] Standing edge waves during beach cusp formation have not been conclusively reported in laboratory or field measurements. Measured phase relationships between subharmonic velocity components at a single alongshore location during one beach cusp formation event are consistent with the presence of standing subharmonic edge waves at the expected frequency [*Huntley and Bowen*, 1973], but such subharmonic signals also can result from interactions between runout and incoming bores [*Emery and Gale*, 1951; *Bascom*, 1951; *Carlson*, 1984; *Mase*, 1988] or from wave groups [*Baldock et al.*, 1997]. The edge wave model only predicts the steady-state spacing of the beach cusps, but not their temporal evolution. It does not specifically address patterns of erosion and deposition [*Guza and Bowen*, 1981], but rather only patterns of fluid flow preceding beach cusp formation. Field measurements of run-up coincident with beach cusp formation have not revealed detectable standing edge waves [*Holland and Holman*, 1996; *Masselink and Pattiaratchi*, 1998; *Burnet*, 1998].

[6] In the self-organization model, beach cusps are initiated by positive feedbacks between flow and morphology and are stabilized by negative feedbacks [*Werner and Fink*, 1993]. Swash flow decelerates and deposits sediment when running up the beach and accelerates and erodes sediment when running down the beach. Run-up diverging on rises leads to net deposition, whereas run-down converging in depressions leads to net erosion, resulting in unstable perturbations of a laterally flat beach under a range of conditions, if sediment flux depends nonlinearly on flow velocity. Numerical models with sediment flux proportional to a power of flow velocity give rise to the formation of patterns resembling beach cusps [*Werner and Fink*, 1993; *Coco et al.*, 2000].

[7] In the self-organization model, beach cusps become stable through negative feedbacks as bay curvature, which controls the inward and outward routing of water, evolves to a value for which flow circulates at constant velocity. As a consequence, sediment flux gradients tend to zero (sediment is neither eroded nor deposited), allowing for steady-state of the cuspate features. A scaling argument yields a linear relationship between beach cusp spacing and swash excursion, if sediment flux varies as the cube of flow velocity. Both edge wave and self-organization models lead to similar predictions for beach cusp spacing, because of a
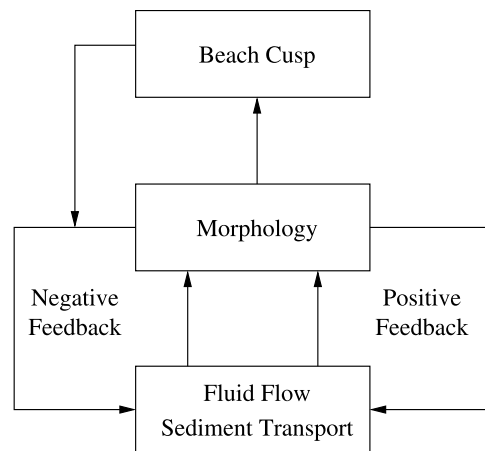

Figure 1. Sketch of feedbacks in beach cusp formation.

relationship between swash excursion and incident wave period enforced by saturation of swash flow in the wind-wave frequency band [*Werner and Fink*, 1993; *Coco et al.*, 1999].

[8] Here, detailed tests of a numerical implementation of the self-organization model are conducted. Specifically, signatures of positive and negative feedbacks in field observations are compared with corresponding signatures in numerical simulations.

2. Signatures of Self-Organization

[9] As beach cusps begin to form by self-organization, a positive feedback that enhances relief develops between morphology on the one hand and fluid flow and sediment transport on the other hand (Figure 1). This feedback is asymmetrical because morphology responds slowly (timescale minutes to hours), thereby controlling flow and transport patterns, which respond quickly (timescale seconds) [*Werner*, 1999]. As a well-defined, even slower (timescale tens of hours to days) responding beach cusp emerges, a negative feedback between flow, morphology and sediment transport develops that opposes beach cusp growth.

[10] On a planar beach with no net erosion, sand deposited uniformly by run-up is eroded uniformly by run-down. The initial growth in relief of a beach cusp is caused by the effect of morphology on flow. Specifically, swash is diverted from incipient horns to incipient bays, leaving residual deposition on horns and leading to enhanced erosion in bays. Three signatures of this positive feedback during the growth of beach cusps are that swash flow increasingly is affected by morphology, swash flow increasingly is diverted from horns to bays, and both deposition on horns and erosion in bays increase.

[11] The first two of these positive feedbacks affect the time that swash front (leading edge of swash flow) motion in bays lags behind swash front motion on horns. This time lag, which is measurable, originates with three mechanisms: (1) If confined to cross-shore motion, swash flow returns in less time on a steep horn than in a shallow bay; (2) the alongshore flow of swash into a bay delays the run-down in that bay; and (3) run-down in a bay can interact with and delay run-up from the next collapsing bore in that bay.

[12] The time lag from the first of these delay mechanisms, owing to differing slopes, can be calculated analytically by idealizing the swash front as a particle constrained to move (without friction) up and down cross-shore lines with constant slope. The time for such a particle to return to its launching point is $T_i = 2v_0/(g\beta_i)$, with v_0 its initial velocity up the beach, β_i the cross-shore slope at profile i, and g the acceleration of gravity. The resulting time lag between the bay (b) and horn (h) of a beach cusp, ΔT, is half the difference $T_b - T_h$, if the phase of the swash starting up the beach is assumed to be uniform alongshore. This time lag can be related to the mean beach cusp height, H_{bc}, if $\beta_i \ll 1$,

$$\frac{\Delta T}{\langle T \rangle} = \frac{(\beta_h - \beta_b)}{2\beta_b\beta_h\langle\frac{1}{\beta}\rangle} \simeq \frac{H_{bc}}{2\beta_b H_s\langle\frac{1}{\beta}\rangle}, \quad (1)$$

where $\langle\frac{1}{\beta}\rangle$ is the mean inverse beach slope, $\langle T \rangle$ is the mean return time for a particle, and H_s is the vertical swash excursion $v_0^2/2g$. When the difference between the slopes of the horn and bay are small compared with the mean slope (e.g., for small amplitude beach cusps), the nondimensional time lag can be simplified to

$$\frac{\Delta T}{\langle T \rangle} = \frac{\beta_h - \beta_b}{2\langle\beta\rangle} \simeq \frac{H_{bc}}{2H_s}. \quad (2)$$

[13] The delay caused by diversion of swash from horns to bays is more difficult to quantify, but the circulation time for diverted swash can be approximated as the time it takes to go up the horn and down the bay plus the time required to travel from horn to bay, $T_{total} = T_h/2 + T_b/2 + T_{div}$. When H_{bc} is small and diverted flow is negligible, T_{div} can be large, because the horn-bay slope difference driving the flow is small. When H_{bc} is large and significant flow is diverted, T_{div} is small. In the former case, the bay-horn time lag should be unaffected because the larger cross-shore slope drives the run-down to the next bore before it flows to the bay. In the latter case, the bay-horn time lag should be unaffected because the circulation time for the diverted flow, driven by a high alongshore slope, probably is less than that for swash originating in bays.

[14] The third mechanism, the delay caused by collisions between incoming bores and enhanced outgoing swash in bays, also is difficult to quantify, but is likely to actually decrease horn-bay time lags. Such collisions might delay the onset of run-up, but, perhaps more significantly, collisions would decrease the initial kinetic energy of the swash, thereby decreasing T_b. A decrease in time lags also might originate from the cross-shore shape of the beach profile (generally convex at horns and concave at bays). Assuming a simplified configuration of the horn and bay profiles such that the only difference is the profile concavity (but the length, as well as the initial and final elevations are the same), it follows that swash running down the concave bay is faster than swash running down the convex horn. For the swash front positioned at any point on the cross-shore profile, swash velocity increases as the square root of the difference in elevation between the initial and current swash front position. This difference, apart from the initial and final point of the profile, always is larger on a concave

profile, implying that the effect of the profile concavity is to decrease the time lag of swash front motion in bays behind that in horns (owing to differences in slope, as discussed above).

[15] A second signature of positive feedback is the effect of increasing beach cusp height (and therefore of time lags between horns and bays) on deposition (horns) and erosion (bays) rates. As flow diversions increase with increasing beach cusp height, the differential rate of deposition between horns and bays should increase, in the absence of negative feedback. However, with increasing beach cusp height, the ability of diverted flow to deposit sediment on horns and erode it from bays is diminished because flow increasingly circulates at constant velocity through the beach cusp [*Werner and Fink*, 1993]. Therefore, the differential rate of morphological change between horns and bays initially should rise with increasing flow diversion (measured through time lags), and then decrease to zero as beach cusps stabilize. An analytical expression for the dependence of morphological evolution on flow diversion is lacking, but it can be calculated with numerical simulations.

[16] In summary, if beach cusps form by self-organization, time lags between bay and horn swash front motions should increase with increasing beach cusp height and the difference between rates of morphological change on horns and bays initially should rise owing to positive feedback and then fall owing to negative feedback. These signatures of self-organization do not include a direct accounting of flow diversion, which is difficult to measure. Here, the self-organization model is tested by searching for these qualitative signatures during beach cusp formation and by comparing the results quantitatively with numerical simulations.

3. Experiment Description

[17] Three experiments were performed in which beach cusps formed on an ocean beach at the Army Corps Field Research Facility in Duck, North Carolina. The beach faces 20deg north of east and the mean sediment diameter is approximately 0.45 mm [*Birkemeier et al.*, 1985]. The average foreshore slope is about 0.1 following prolonged periods of small waves and is lower during storms. Two Nor'easter storms bracketed the three experiments (Figures 2–3).

[18] In experiment A, a Nor'easter storm generated waves with surf zone significant wave heights exceeding 1 m and alongshore currents from the north exceeding 0.6 m/s (3–4 September, Figure 2) that planed beach cusps with approximately 25 m spacing and 0.25 m maximum height and reduced the foreshore slope to 0.085 (Figures 3–4). New beach cusps began to form at high tide at the end of 4 September. As waves and currents from the storm began to subside, these beach cusps grew to a 0.25 m maximum height with 35 m spacing on the morning of 5 September. Under waves with 0.5 m significant height and an alongshore current less than 0.1 m/s, beach cusps evolved to 0.5 m maximum height with 22 m spacing by 8 September (Figure 4). In experiment B, beach cusps formed after a bulldozer was used to reduce the maximum height of three beach cusps with about 30 m spacing from 0.75 m to less than 0.2 m on 11 September. (Surveys were not performed immediately after bulldozing was completed and before the
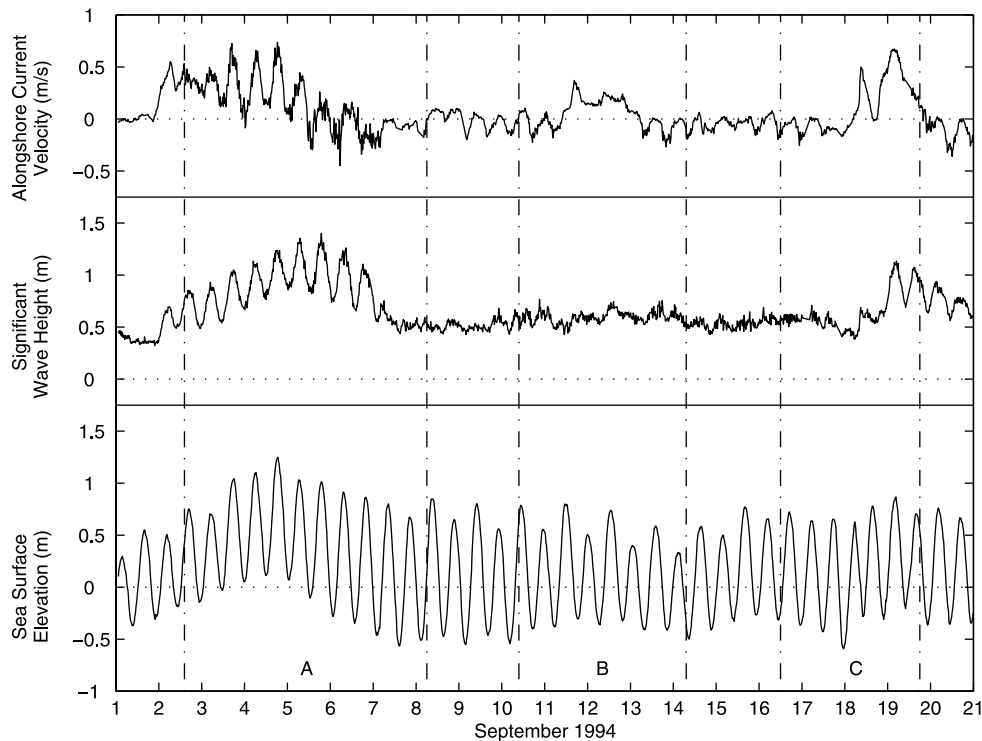
Figure 2. Alongshore current, significant wave height, and sea surface elevation (relative to mean sea level) versus time. Storm waves bracketed a set of three experiments (A, B, and C). The end of experiment A, experiment B, and the beginning of experiment C were characterized by smaller waves and currents, with slightly higher currents in the middle of experiment B. Values are averages over 1024 s from a colocated pressure gauge and current meter in approximately 2 m mean water depth.

rising tide began to transport sand on the smoothed section of beach. Therefore, the extent to which beach cusps were planed is somewhat uncertain.) These beach cusps were planed on a 90-m stretch of beach that was a control for an adjacent section that also was planed and into which channels of different depths were excavated. With a significant wave height of 0.6 m driving an alongshore current of less than 0.1 m/s (Figure 2), beach cusps reformed to 0.35 m maximum height with 30 m spacing by 12 September (Figure 4). The horns of these beach cusps originally pointed to the north, but then rotated to the south by 13 September (Figures 3–4). In experiment C, beach cusps formed after a bulldozer was used to reduce the maximum height of three beach cusps with about 30 m spacing from 0.5 m to less than 0.1 m at noon on 17 September. With a significant wave height of 0.6 m and an alongshore current less than 0.1 m/s (Figure 2), beach cusps rapidly reformed to 0.5 m maximum height with 30 m spacing by the evening of 17 September (Figure 4). On 19 September, a Nor'easter storm, with surf zone significant heights exceeding 1 m driving an alongshore current from the north exceeding 0.6 m/s (Figure 2) planed the beach and reduced the foreshore slope to 0.07 by erosion, resulting in a steep scarp most prominent at the former location of beach cusp horns (Figure 3).

4. Measurement Techniques

[19] Measurements of morphology and flow in shallow water are required because feedbacks between swash flow and morphology are largest at the shoreline. Beach mor-

phology was measured continuously with theodolite surveys on an approximate grid with 5 m spacing at 3- to 4-hour intervals over a region encompassing the upper beach and the swash zone, extending approximately 60 m cross shore and 100 to 200 m alongshore. Raw measurements were translated and rotated into a common coordinate system and interpolated onto a uniform grid. The vertical uncertainty in interpolated points owing to technician error, theodolite tilt, and finite sampling is estimated to be 0.03–0.05 m, based on measured differences in beach height from survey to survey on the upper beach, where the elevation remained fixed.

[20] Motion of the swash front was measured from video-tape images [e.g., *Holland and Holman*, 1993] recorded continuously during daylight hours from a tower located approximately 300 m alongshore, 80 m inland, and 40 m above the surveyed regions. Digitized images with 640 × 480 1-byte pixels were sampled at 0.5-s intervals from 2-hour videotapes. Pixels along cross-shore profiles spaced 5 m apart were extracted from images using a transformation based on surveyed morphology and circular fiducial points in the image (following *Holland and Holman* [1993]). The centroids of fiducial points (located through their contrast in brightness with the surroundings) were tracked on each image to correct for an up to 5-pixel variation in camera aim owing to tower sway from turbulent storm winds.

[21] The swash front is located as the intersection of white foam from breaking waves in the run-up and darker beach sand using an empirical algorithm (see *Burnet* [1998] for details). The swash front on a cross-shore line is detected
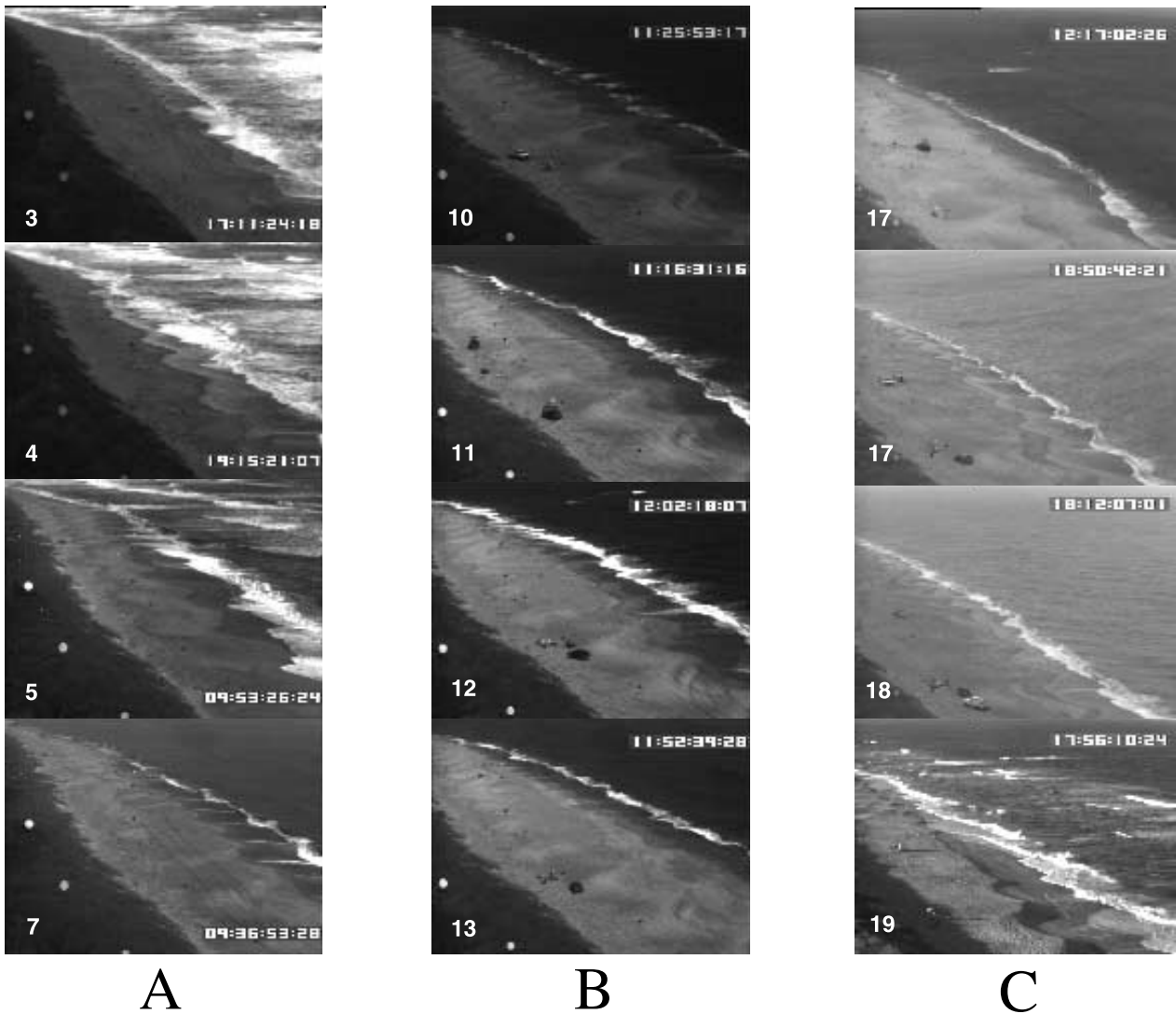
Figure 3. Video images of the beach during experiments A, B, and C. The date in September is indicated in the upper or lower left corners and time (local) is indicated in the upper right corners. The dark area (on the left of each image) is above the high tide level. Swash at the shoreline appears as bright white (from upper left to lower right of each image). Northerly sea and swell dominate in experiment A, whereas southerly swell is combined with small, oblique waves from the north in experiments B and C (see Figure 2).

automatically where pixel brightness (0–255) seaward of exposed beach sand exceeds a threshold brightness level $B_t = B_{sand} \times (2 - B_{sand}/B_{light})$, where $B_{sand} = (B_{dark} + B_{const})/2$, B_{dark} and B_{light} are the lowest and the highest average brightness of a group of pixels along a cross-shore line, respectively, and B_{const} is a constant parameter between 70 and 200 (typically ~100) that tends to be proportional to the swash zone brightness averaged over a 2-hour videotape. Uncertainty in swash front elevation is estimated to be approximately 0.05 m, based on pixel size and uncertainty in beach elevation (but not including errors in tracking the swash front position). Occasionally, this algorithm failed to track the swash front, mostly when lighting conditions were poor or when run-up infiltrated significantly into the beach. Failures at isolated points were corrected manually. One videotape from the middle and six videotapes from the end

of experiment A and 2 videotapes from experiment B were discarded because they contain extended series of tracking failures.

5. Analysis

[22] Time lags are calculated as the peak in the cross correlation of swash front elevation time series measured along two cross-shore profiles. The evaluation of the cross correlation peak was performed using a cubic interpolation of the 2-Hz measurements with a 4-Hz mesh. The time lags are not sensitive to mesh size below this value. Coherence of swash front elevation between bays and horns is generally high, with mean greater than 0.8 and the lowest value greater than 0.5. A maximum uncertainty in time lag of 0.075 s (95%) was estimated from simulated time series.
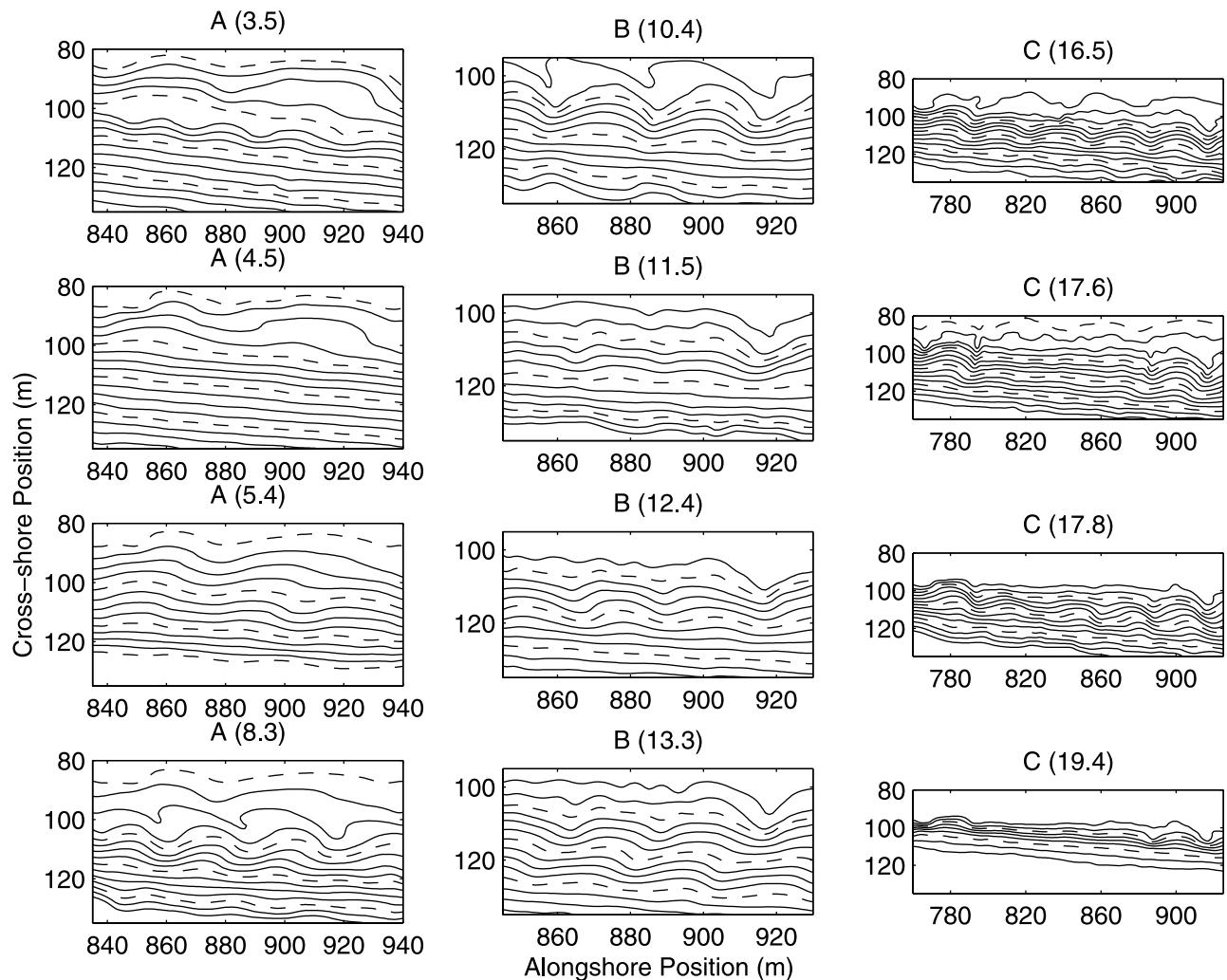
Figure 4. Measured beach morphology during experiments A, B, and C. Numbers in parentheses indicate the start time of surveys given by September date. Contour interval is 0.5 m. Beach cusps form (5.4) after a Nor'easter storm planed (4.5) the beach in experiment A. Beach cusps re-formed (12.4 and 17.8) after the beach was planed with a bulldozer (11.5 and 17.6) in experiments B and C. A second Nor'easter storm planed (19.4) the beach at the end of experiment C.

Specifically, statistical fluctuations were calculated for time lags between a measured time series and the same time series with a lag and to which low-passed ($0-0.2$ Hz) white noise with standard deviation 1.7 m was added so that the two time series had a coherence between bays and horns of about 0.5, close to the lowest value in the observations.

[23] Morphological changes were evaluated inside a region bounded by the position of the mean swash front and the mean plus 2 standard deviations (the area where the most significant morphological changes were observed and where surveys could be performed at all tidal levels). Beach cusp height is calculated as the largest difference between the maximum and the minimum elevation along a line spanning two beach cusp horns, parallel to the mean swash front position and ranging, in the cross-shore, between the mean swash front and the mean plus 2 standard deviations. The beach slope at a given alongshore position is estimated from the slope of a linear least squares fit to the surveyed points between the mean cross-shore position of the swash front and the mean plus 2 standard deviations. For calculat-

ing time lags in both the measurements and the model, the positions of horns and bays were determined from zero-crossings in graphs of time lag versus alongshore position.

6. Model Description

[24] Predictions of the self-organization model were calculated using modifications of an existing numerical model (*Coco et al.* [2000] after *Werner and Fink* [1993]). The motion of the swash front, sediment transport, and resulting morphological change were simulated with frictionless, sediment-carrying water particles confined to the beach surface, the trajectories of which were determined by initial velocity, morphology, and gravity.

[25] The model was initialized with measured beach morphology interpolated onto a 0.5 by 0.5 m grid. For those surveys that did not extend from the lowest to the highest swash front positions, measured morphology was extended assuming a linear slope equal to the average surveyed cross-shore slope. To reduce the effect of lateral
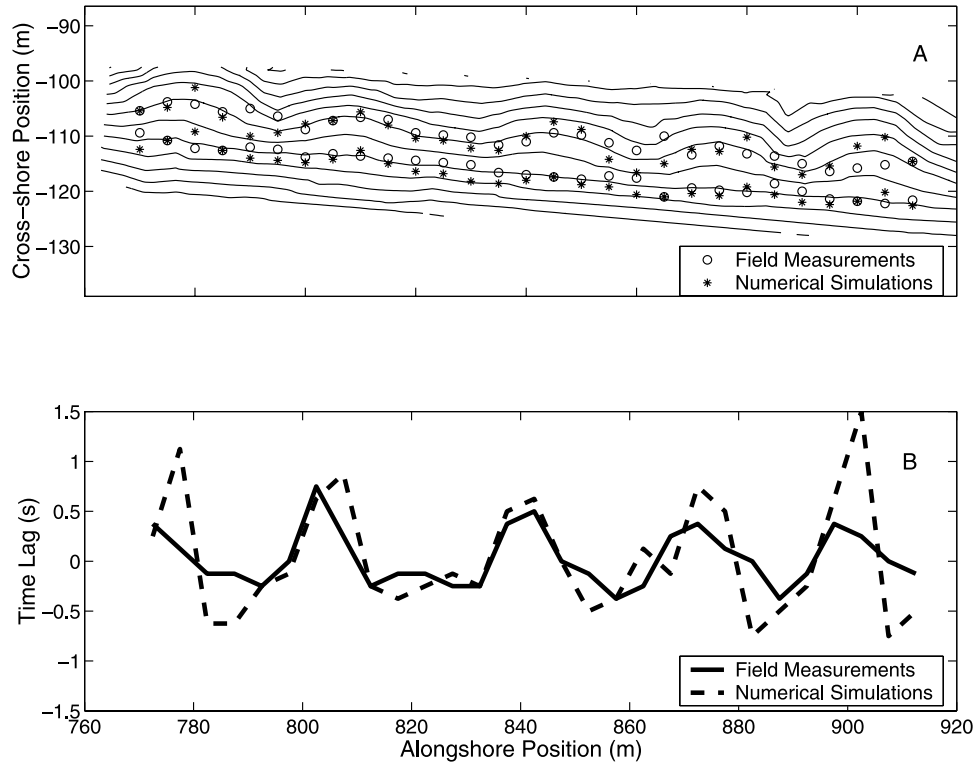
Figure 5. (a) Measured beach morphology (contour interval 0.25 m) during experiment C (September 18 at 17.45) and observed (circles) and predicted (asterisks) position of the mean swash front and of the mean swash front position plus 2 standard deviations. (b) Time lag versus alongshore distance for field measurements (solid curve) and numerical simulations (dashed curve) calculated from cross-correlation of swash front time series between adjacent cross-shore transects for 17.45–19.45 on September 18.

boundaries in the numerical simulations, the surveyed morphology was mirrored twice and periodic boundary conditions were employed.

[26] A swash cycle is defined from h_0, a local minimum in the measured swash height time series $h(t)$, to a maximum, $h_0 + \Delta h$ (with Δh required to be greater than 1 standard deviation of $h(t)$), to the next minimum. The vertical swash excursion (Δh) and the swash height at the beginning of a cycle (h_0) are not independent; therefore, a coupled distribution of swash front elevation h_0 and cross-shore velocity of water particles v_0 was derived from $h(t)$ and used to choose a sequence of (uncorrelated) initial conditions for each modeled swash cycle. The initial velocity is calculated as $v_0 = \sqrt{2g\Delta h}$.

[27] Water particles are launched at an angle relative to shore normal that is the inverse tangent of the ratio of the initial water particle velocity to the alongshore velocity at the point where the collapsing bore begins to move up the beach, estimated from the alongshore trend of time lags in $h(t)$. This calculation accounts for large bores, but neglects additional smaller bores propagating at higher angles that sometimes are visible in videotapes. In the model, the vertical amplitude of swash flow is independent of along-shore position, because the swash front is modeled with energy-conserving, kinematical particles.

[28] The numerically simulated swash positions were sampled for 2-hour periods at 2 Hz along cross-shore profiles spaced 5 m apart, corresponding to the sampling of the field observations. Swash position was determined from the highest water particle in the 5-m swath surrounding the profile. In one set of numerical simulations (used to analyze how developing morphology affects the flow), bed elevations were fixed at the interpolated surveyed morphology. In a second set of numerical simulations (used to analyze how flow affects morphology), morphology was initialized with interpolated measurements and then allowed to change through erosion and deposition of sediment by water particles. The carrying capacity of water particles is proportional to the square of their velocity, corresponding to a cubic dependence of sediment flux on the flow velocity.

7. Results

[29] Field observations of swash motions exhibit the influence of morphology on flow, which is one component of positive feedback between flow and morphology. In addition to this qualitative signature of self-organization, the measurements are in quantitative agreement with predictions from the numerical model using measured bathymetry. On well-developed beach cusps at high tide, observed and modeled time lags coincide within statistical uncertainties (Figure 5). More generally, both observed and modeled time lags increase with increasing beach cusp height (Figure 6 and Table 1) and increasing difference between horn and bay cross-shore slopes (Figure 7 and Table 2). The relatively small number of points in Figures 6 and 7 is related to the difficulty of finding exact correspondence between the hydrodynamics (only
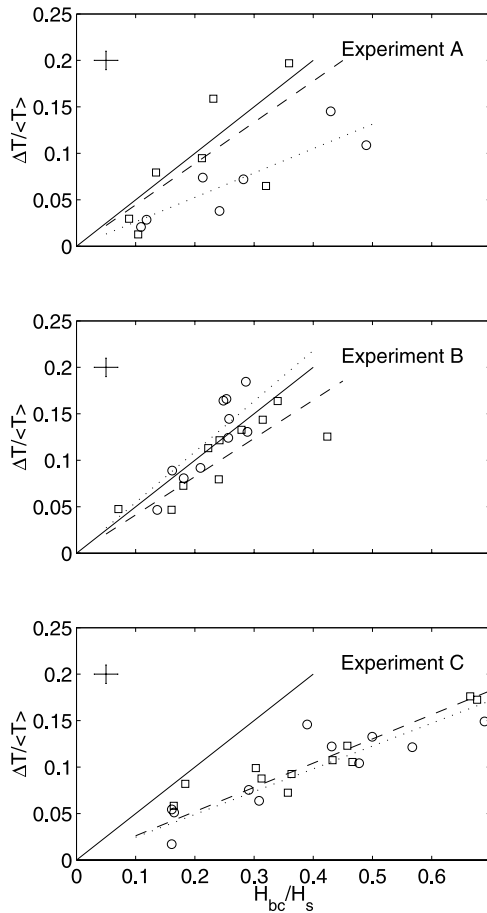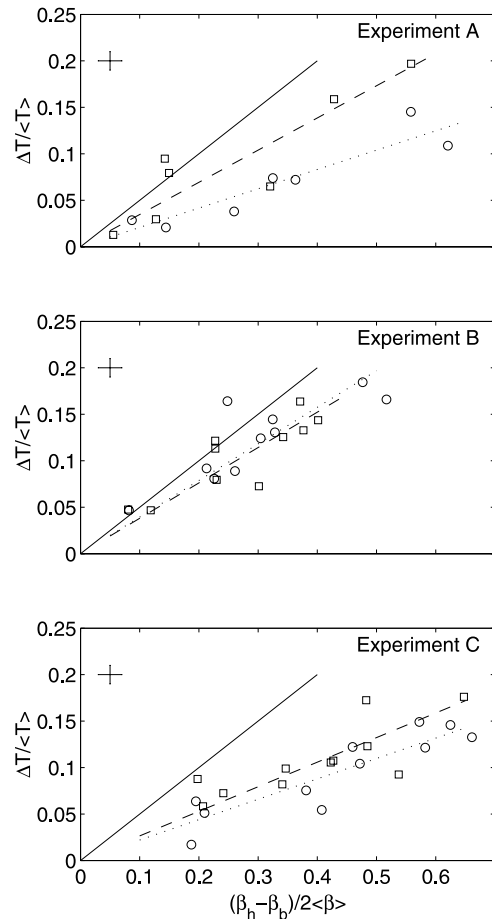
Figure 6. Normalized bay-to-horn time lag versus normalized beach cusp height for field measurements (circles) and numerical simulations (squares) for Experiments A, B, and C. Solid line is prediction from equation (2), and the dotted and dashed lines are field and numerical model best fit regressions (see Table 1), respectively. Statistical uncertainties (upper left corner) are estimated to be 0.02 for the beach cusp height parameter and 0.01 for dimensionless time lags.
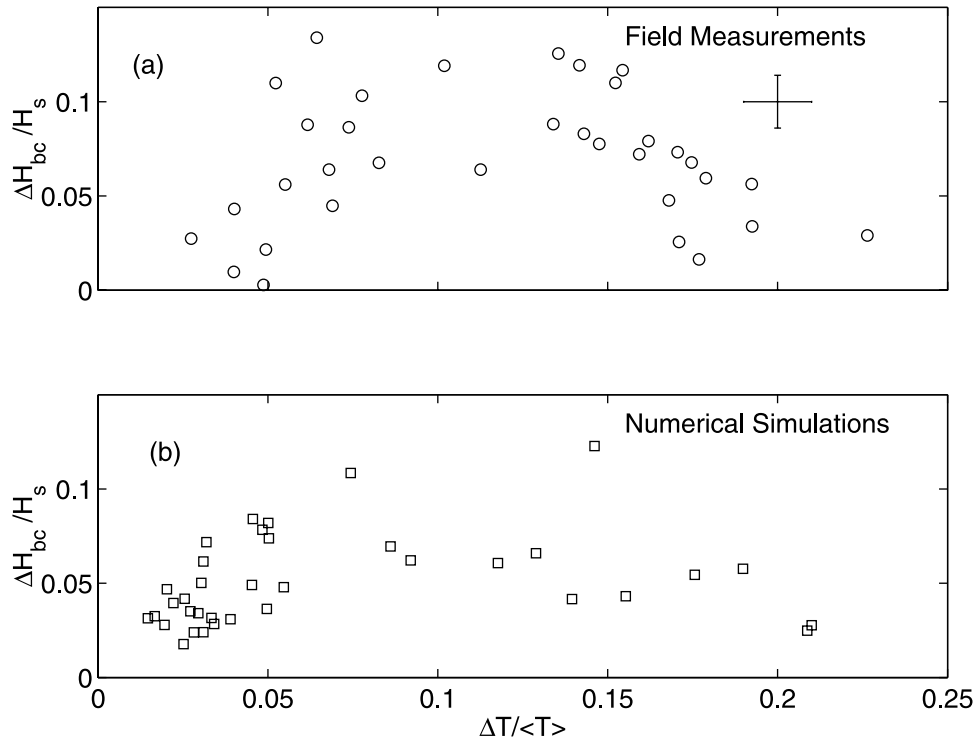
Figure 7. Normalized bay-to-horn time lag versus normalized horn-to-bay slope difference for field measurements (circles) and numerical simulations (squares) for Experiments A, B, and C. Solid line is prediction from equation (2), and the dotted and dashed lines are field and numerical model best fit regressions (see Table 2), respectively. Statistical uncertainties (upper left corner) are estimated to be 0.02 for the beach cusp slope parameter and 0.01 for dimensionless time lags.

available during daytime) and the surveys. Furthermore, in a few cases, the surveys did not extend far enough offshore to cover the position of the mean swash front, necessary to provide an accurate estimate of the morphological parameters. Such cases have not been included in the analysis unless the available survey indicated the offshore part of the beach was planar and could be estimated by linearly extrapolating measured bathymetry.

Numerical results from beach cusps developing at the lateral boundary of the domain are not included because the modeled flow is affected significantly by the mirrored boundary conditions, especially for small amplitude morphological features. The observed and modeled time lags agree within the statistical uncertainty of the measurements, except for Experiment A where the modeled time lag is correlated with cross-shore slope ($R^2 = 0.80$, Figure 7, Table 2), but not with

Table 1. Slope (m) and Correlation (R^2) From the Linear Regression Between Time Lags and Beach Cusp Height Parameter $\frac{\Delta T}{\langle T \rangle} = m\left(\frac{H_{bc}}{2H_s}\right)$ for Field Observations (F) and Numerical Model Simulations (M)

Experiment	m_F	m_M	R^2_F	R^2_M	95% Level	No. of points
A	0.26	0.44	0.80	0.54	0.57	7
B	0.54	0.41	0.72	0.63	0.40	10
C	0.25	0.26	0.75	0.82	0.36	11

Table 2. Slope (m) and Correlation (R^2) From the Linear Regression Between Time Lags and Cross-Shore Slope Parameter $\frac{\Delta T}{\langle T \rangle} = m\left(\frac{\beta_h - \beta_b}{2\langle \beta \rangle}\right)$ for Field Observations (F) and Numerical Model Simulations (M)

Experiment	m_F	m_M	R^2_F	R^2_M	95% Level	No. of points
A	0.21	0.35	0.86	0.80	0.57	7
B	0.39	0.38	0.62	0.68	0.40	10
C	0.22	0.26	0.81	0.57	0.36	11

Figure 8. Normalized beach cusp height change between sequential surveys (differential erosion between horns and bays) versus (a) normalized bay-to-horn time lag for field measurements and (b) numerical simulations. Statistical uncertainties (bars in Figure 8a) are estimated to be 0.01 for dimensionless time lags and 0.028 for the normalized beach cusp height change.

beach cusp height ($R^2 = 0.54$, not significant at the 95% level, Figure 6, Table 1). The inadequacy of the model in Experiment A might originate in boundary effects (only $2-3$ beach cusps were surveyed) and in the failure to account for coherent low frequency modulation of the swash (which persisted through beach cusp formation following the storm of $4-6$ September) in the numerical model. Moreover, during experiment A beach cusp horns rotated to the north. Although this rotation did not have a significant effect on the time lags, it affected the evaluation of the swash position, which affects the derived quantities shown in Figures 6 and 7.

[30] Time lags from both the field observations and numerical simulations (Figures 6 and 7) are less than kinematical predictions (equation (2)), possibly because cross-shore profiles are convex at horns and concave at bays, both of which result in decreased time lags relative to those on a linear profile assumed in deriving equation (2). Field and numerical results are closest to the theoretical predictions for experiment B, where horns and bays had nearly linear cross-shore profiles.

[31] Another source of discrepancy between observations and predictions is the unmodeled effect of directionally spread waves [*Herbers et al.*, 1999]. Bidirectional waves were observed visually and measured with pressure sensors in the middle of experiment B and at the end of experiment C, but were not incorporated into the initial conditions for water particles beyond the effect of an energy-weighted mean direction determined from alongshore lags in $h(t)$ (section 6).

[32] The second component of positive feedback between flow and morphology, that flow affects morphology change, is investigated with the differential erosion between horns and bays (quantified as the change in beach cusp height over a 2-hour period) as a function of time lag between the swash front in bays and horns. For small normalized time lags $\frac{\Delta T}{\langle T \rangle}$, differential erosion increases with time lag, reaching a peak at $\frac{\Delta T}{\langle T \rangle}$ between 0.10 and 0.15 for both the measurements from the three experiments (Figure 8a) and from a model run initiated with the survey at the beginning of experiment C (Figure 8b). Simulation results obtained from the other two experiments yield similar results. The large scatter in the observations is caused by the uncertainty inherent in a quantity derived from the difference of two surveys, the finite time required to complete a survey ($2-3$ hours), and the frequent divergence of the time at which the time lag was calculated from the midpoint between two surveys. The scatter of the model also stems from uncertainties in initial morphology (surveyed at the beginning of Experiment C), which affects the development of the features under modeled sediment transport. Although there are many possible causes for differences between model predictions and field observations (e.g., simplified sediment transport parameterization, the effect of infiltration, wave direction), measured and modeled differential erosion increase similarly with time lag to a maximum value.

[33] Both observed and modeled differential erosion decrease with further increase in normalized time lag (Figure 8), consistent with negative feedback between flow

and morphology that stabilizes beach cusps at a finite amplitude, a characteristic of the self-organization beach cusp model.

8. Discussion and Conclusions

[34] Self-organization is a general property of many non-linear, dissipative systems. It has been hypothesized to play a significant role in braided rivers [*Murray and Paola*, 1994], sand dunes [*Werner*, 1995], frozen soils [*Kessler et al.*, 2001; *Plug and Werner*, 2001], large-scale coastline development [*Ashton et al.*, 2001], forest fires [*Pastor et al.*, 1999], and insect behavior [*Theraulaz and Bonabeau*, 1995]. In laboratory studies and simulations with numerical models, self-organized dynamics become simpler, less sensitive to detail, and more easily predicted as order increases and timescales become longer. Beach cusp formation involves the nonlinear, dissipative processes of fluid flow and sediment transport; therefore, it is a candidate for exhibiting self-organized behavior, the knowledge of which might lead to increased physical insight and improved predictive capability.

[35] Self-organization as a mechanism for beach cusp formation requires that (1) developing morphology affects the flow of swash and (2) the flow of swash feeds back on sediment transport and morphology change. The relationship between flow and morphology is asymmetrical, because the intrinsic time scale characterizing the evolution of morphology is much longer (minutes to hours) than that of swash flow (seconds). Therefore, as beach cusps develop on a planar beach, the effect of morphology on flow, as measured with lags between flow on horns and bays, should increase monotonically with relief. The effect of flow on morphology change, as quantified by differential erosion between bays and horns, initially should increase as positive feedback causes beach cusps to grow, but then should decrease as negative feedback becomes dominant and beach cusps stabilize. These signatures of self-organization were observed in all three field experiments and were reproduced (within the variability of the measurements) by a numerical model based on self-organization, except for Experiment A, where the modeled lags are noisy and greater than observed lags.

[36] The disparity between modeled and measured swash flow in Experiment A could result from the presence of significant infragravity motions [*Burnet*, 1998] that are not accounted for in the model (where swash characteristics between successive swash cycles are independent), and the failure to survey beach morphology with sufficient cross- and alongshore extent. The scatter in the measurements is caused by uncertainties in morphological change because of the several-hour-long surveys and in swash front measurements, resulting in errors in locating horns and bays. Despite these difficulties, the observations are consistent with the hypothesis that beach cusps form by self-organization.

References

Ashton, A., A. B. Murray, and O. Arnault, Formation of coastline features by large-scale instabilities induced by high-angle waves, *Nature*, *414*, 296–300, 2001.
Baldock, T. E., P. Holmes, and D. P. Horn, Low frequency swash motion by wave grouping, *Coastal Eng.*, *32*, 197–222, 1997.
Bascom, W., The relationship between sand size and beach face slope, *Eos Trans. AGU*, *32*, 866–874, 1951.
Birkemeier, W. A., H. C. Miller, S. D. Wilhelm, A. E. Devall, and C. S. Gorbics, *A User's Guide to the Coastal Engineering Research Center's (CERC's) Field Research Facility*, Natl. Technol. Inf. Cent., Springfield, Va., 1985.
Bowen, A. J., and R. T. Guza, Edge waves and surf beat, *J. Geophys. Res.*, *83*, 1913–1920, 1978.
Bowen, A. J., and D. L. Inman, Edge waves and crescentic bars, *J. Geophys. Res.*, *76*, 8662–8671, 1971.
Burnet, T. K., Field testing two beach cusp formation models, Ph.D. thesis, Duke Univ., Durham, N. C., 1998.
Carlson, C., Field studies of run-up on dissipative beaches, paper presented at 19th International Conference of Coastal Engineering, Am. Soc. of Civ. Eng., Reston, Va., 1984.
Coco, G., T. J. O'Hare, and D. A. Huntley, Beach cusps: A comparison of data and theories for their formation, *J. Coastal Res.*, *15*, 741–749, 1999.
Coco, G., D. A. Huntley, and T. J. O'Hare, Investigation of a self-organisation model for beach cusp formation and development, *J. Geophys. Res.*, *105*, 21,991–22,002, 2000.
Dalrymple, R. A., and G. E. Lanan, Beach cusp formed by intersecting waves, *Geol. Soc. Am. Bull.*, *87*, 57–60, 1976.
Dean, R. G., and E. M. Maurmeyer, Beach cusps at Point Reyes and Drakes Bay Beaches, California, paper presented at 17th International Conference of Coastal Engineering, Am. Soc. of Civ. Eng., Sydney, Australia, 1980.
Dubois, R. N., Beach topography and beach cusps, *Geol. Soc. Am. Bull.*, *89*, 1133–1139, 1978.
Emery, K., and J. Gale, Swash and swash marks, *Eos Trans. AGU*, *32*, 31–36, 1951.
Gallagher, B., Generation of surf beat by nonlinear wave interaction, *J. Fluid Mech.*, *49*, 1–20, 1971.
Guza, R. T., and A. J. Bowen, On the amplitude of beach cusps, *J. Geophys. Res.*, *86*, 4125–4132, 1981.
Guza, R. T., and R. E. Davis, Excitation of edge waves by waves incident on a beach, *J. Geophys. Res.*, *79*, 1285–1291, 1974.
Guza, R. T., and D. Inman, Edge waves and beach cusps, *J. Geophys. Res.*, *80*, 2997–3012, 1975.
Herbers, T. H. C., S. Elgar, and R. T. Guza, Generation and propagation of infragravity waves, *J. Geophys. Res*, *100*, 24,863–24,872, 1995.
Herbers, T. H. C., S. Elgar, and R. T. Guza, Directional spreading of waves in the nearshore, *J. Geophys. Res.*, *104*, 7683–7693, 1999.
Holland, K. T., and R. A. Holman, The statistical distribution of swash on natural beaches, *J. Geophys. Res.*, *98*, 10,271–10,278, 1993.
Holland, K. T., and R. A. Holman, Field observations of beach cusps and swash motions, *Mar. Geol.*, *134*, 77–93, 1996.
Huntley, D. A., and A. J. Bowen, Field obsevations of edge waves, *Nature*, *243*, 160–163, 1973.
Inman, D. L., and R. T. Guza, The origin of swash cusps on beaches, *Mar. Geol.*, *49*, 133–148, 1982.
Kessler, M. A., A. B. Murray, B. T. Werner, and B. Hallet, A model for sorted circles as self-organized patterns, *J. Geophys. Res.*, *106*, 13,287–13,306, 2001.
Komar, P., Observations of beach cusps at Mono Lake, California, *Geol. Soc. Am. Bull.*, *84*, 3593–3600, 1973.
Kuenen, P. H., The formation of beach cusps, *J. Geol.*, *97*, 34–40, 1948.
Longuet-Higgins, M. S., and D. W. Parkin, Sea waves and beach cusps, *Geogr. J.*, *128*, 194–200, 1962.
Mase, H., Spectral characteristics of random wave run-up, *Coastal Eng.*, *12*, 175–189, 1988.
Masselink, G., and C. B. Pattiaratchi, Morphological evolution of beach cusp morphology and associated swash circulation patterns, *Mar. Geol.*, *146*, 93–113, 1998.
Masselink, G., B. J. Hegge, and C. B. Pattiaratchi, Beach cusp morphodynamics, *Earth Surf. Processes Landforms*, *22*, 1139–1155, 1997.
Miller, J. R., S. M. O. Miller, C. A. Torzynski, and R. C. Kochel, Beach cusp destruction, formation, and evolution during and subsequent to an extratropical storm, Duck, North Carolina, *J. Geol.*, *97*, 749–760, 1989.

Murray, B., and C. Paola, A cellular model of braided rivers, *Nature*, *371*, 54–57, 1994.

Pastor, J., Y. Cohen, and R. Moen, Generation of spatial pattern in boreal forest landscapes, *Ecosystems*, *2*, 439–450, 1999.

Plug, L. J., and B. T. Werner, Fracture networks in frozen grounds, *J. Geophys. Res.*, *106*, 8599–8613, 2001.

Russell, R. J., and W. G. McIntire, Beach cusps, *Geol. Soc. Am. Bull.*, *76*, 307–320, 1965.

Sallenger, A. H., Beach cusp formation, *Mar. Geol.*, *29*, 23–37, 1979.

Theraulaz, G., and E. Bonabeau, Coordination in distributed building, *Science*, *269*, 686–688, 1995.

Ursell, F., Edge waves on a sloping beach, *Proc. R. Soc. London, Ser. A*, *214*, 79–97, 1952.

Werner, B. T., Eolian dunes: Computer simulations and attractor interpretation, *Geology*, *23*, 1107–1110, 1995.

Werner, B. T., Complexity in natural landform patterns, *Science*, *284*, 102–104, 1999.

Werner, B. T., and T. M. Fink, Beach cusps as self-organized patterns, *Science*, *260*, 968–971, 1993.

Williams, A., The problem of beach cusp development, *J. Sediment. Petrol.*, *43*, 33–52, 1973.

———————————

T. K. Burnet and B. T. Werner, Complex Systems Laboratory, Cecil and Ida Green Institute of Geophysics and Planetary Physics, University of California, San Diego, La Jolla, CA 92093-0225, USA. (bwerner@ucsd.edu)

G. Coco, National Institute of Water and Atmospheric Research, P.O. Box 11-115, Hamilton, NZ. (g.coco@niwa.co.nz)

S. Elgar, Woods Hole Oceanographic Institution, Woods Hole, MA 02543, USA. (elgar@whoi.edu)